

Research Article

Open Access



Near-room-temperature reversible switching of quadratic optical nonlinearities in a one-dimensional perovskite-like hybrid

Qingshun Fan^{1,2}, Yu Ma¹, Haojie Xu^{1,2}, Yipeng Song¹, Yi Liu¹, Junhua Luo^{1,2,3} , Zihua Sun^{1,2,3} 

¹State Key Laboratory of Structural Chemistry, Fujian Institute of Research on the Structure of Matter, Chinese Academy of Sciences, Fuzhou 350002, Fujian, China.

²College of Materials Science and Opto-Electronic Technology, University of Chinese Academy of Sciences, Chinese Academy of Sciences, Beijing 100039, China.

³Fujian Science & Technology Innovation Laboratory for Optoelectronic Information of China, Fuzhou 350108, Fujian, China.

Correspondence to: Prof. Zihua Sun, State Key Laboratory of Structural Chemistry, Fujian Institute of Research on the Structure of Matter, Chinese Academy of Sciences, 155 Yangqiao W Rd., Gulou District, Fuzhou 350002, Fujian, China.
E-mail: sunzihua@fjirsm.ac.cn

How to cite this article: Fan Q, Ma Y, Xu H, Song Y, Liu Y, Luo J, Sun Z. Near-room-temperature reversible switching of quadratic optical nonlinearities in a one-dimensional perovskite-like hybrid. *Microstructures* 2022;2:2022013.
<https://dx.doi.org/10.20517/microstructures.2022.09>

Received: 26 Apr 2022 **First Decision:** 16 May 2022 **Revised:** 22 May 2022 **Accepted:** 30 May 2022 **Published:** 16 Jun 2022

Academic Editor: Shujun Zhang **Copy Editor:** Fangling Lan **Production Editor:** Fangling Lan

Abstract

The switching of quadratic nonlinear optical (NLO) effects between two or more NLO states of solid-state materials represents an intriguing new branch in the field of photoelectrics and optics. While structural phase transitions have shown potential in this field, near-room-temperature reversible NLO switches have rarely been reported. To exploit new NLO switching materials within the structurally flexible class of hybrid perovskites, here, we synthesize a one-dimensional perovskite-like hybrid, (MP)PbBr₃ (where MP⁺ is a 1-methylpyrrolidinium cation), through a facile solution method, which exhibits strong second harmonic generation (SHG) activities with an intensity of ~1.6 times as large as potassium dihydrogen phosphate. Intriguingly, (MP)PbBr₃ enables the near-room-temperature reversible switching of SHG properties, showing a large NLO switching contrast of up to ~40 between its SHG-active and SHG-inactive phases, beyond most of its liquid counterparts. Further microscopic structural analyses reveal that the dynamic ordering of the organic MP⁺ cation and inorganic chain-like skeleton triggers its centrosymmetric (*P6₃/mmc*) to acentric (*P2₁2₁2₁*) phase transition at 316 K upon cooling, resulting in a crucial contribution to its NLO switching properties. This work illustrates the potential of this material as a candidate for solid-state NLO switches and will promote the development of NLO materials within the family of low-dimensional hybrid perovskites.



© The Author(s) 2022. **Open Access** This article is licensed under a Creative Commons Attribution 4.0 International License (<https://creativecommons.org/licenses/by/4.0/>), which permits unrestricted use, sharing, adaptation, distribution and reproduction in any medium or format, for any purpose, even commercially, as long as you give appropriate credit to the original author(s) and the source, provide a link to the Creative Commons license, and indicate if changes were made.



Keywords: Phase transition, nonlinear optical properties, NLO switching, hybrid perovskites

INTRODUCTION

Solid-state crystalline materials that enable the switching of nonlinear optical (NLO) properties between two or more states under external stimuli, such as light, heat, and pressure, have been attracting considerable attention for their potential applications in photoswitches, biosensors, environment monitors, and memory storage^[1-4]. For liquid systems, the switching of NLO properties has been achieved through chemical modifications, such as redox reactions, protonation, and photochromism^[5-7]. However, realizing the high reversibility of NLO switching in liquids remains a challenge because they face serious detuning or instability problems. In contrast, solid-state NLO materials that show the controllable second harmonic generation (SHG) signal between different phases offer a potential platform for achieving excellent NLO switching behavior^[8,9]. The SHG-active phase is generally known as the “SHG-on” state, while the SHG-inactive phase corresponds to the “SHG-off” state. In this regard, the thermally-induced structural phase transition from a non-centrosymmetric (NCS) phase to a centrosymmetric (CS) structure might be effective in triggering switchable SHG properties in solid-state crystalline materials^[10]. Several typical solid-state materials that exhibit switchable NLO behaviors have so far been reported, such as single-component plastic crystals^[11], host-guest inclusion compounds^[12], organic-inorganic hybrids^[13], covalent organic frameworks^[14], and ionic salts^[15]. These compounds undergo structural changes with different phase transition temperatures (T_c), such as $[\text{NH}_3(\text{CH}_2)_5\text{NH}_3]\text{SbCl}_5$ (365.4 K)^[16], $(\text{C}_6\text{H}_{14}\text{N})_2\text{SbCl}_5$ (477 K)^[17], $[(\text{CH}_3)_3\text{PCH}_2\text{OH}][\text{Cd}(\text{SCN})_3]$ (248.5 K)^[18] and $[(\text{CH}_3)_4\text{P}]_2\text{Cr}_2\text{O}_7$ (221 K)^[19], in which the SHG responses display remarkable variations. Despite the reasonable development of phase transition materials, near-room-temperature reversible NLO switches have rarely been reported. Hence, there is an urgent need to explore new NLO switching materials that undergo the NCS-to-CS phase transition near room temperature.

Organic-inorganic hybrid perovskites provide a significant opportunity to combine phase transitions with multiple switching responses^[20]. Compared with purely inorganic or organic materials, hybrid perovskites combine the advantages of inorganic networks and organic components into a single-phase structure to achieve multifunctional properties^[21-23]. Among them, the low-dimensional perovskites derived from the 3D ABX_3 -type prototype have also attracted significant interest because of their structural flexibility and diversity in triggering dynamic phase transitions^[24,25]. Structurally, large-sized organic components can easily be accommodated to form low-dimensional perovskites [e.g., zero-, one-dimensional (1D) and two-dimensional (2D) subclasses], which possess considerable freedom of dynamic motion. Under external stimuli, the flexible organic cations may undergo rotations or reorientations that afford a driving force to structural phase transitions^[26,27]. Consequently, low-dimensional hybrid perovskites have been regarded as ideal platforms for constructing solid-state phase transition materials^[28-30]. For instance, Ai *et al.* reported a 1D perovskite-like hybrid of (trimethylchloromethylammonium) CrCl_3 , in which the ordering of the organic cations leads to a ferroelectric-type phase transition along with notable SHG properties^[31]. Considering their structural flexibility and diversity, it is believed that low-dimensional hybrid perovskites provide tremendous opportunities to induce phase transitions and explore new materials for NLO switches.

The pyrrolidine ring is an important building block that has been exploited as a dynamic source to assemble phase transition materials, as exemplified by ferroelectrics and switchable dielectrics^[32,33]. Under thermal stimuli, pyrrolidine moieties can spontaneously assemble into a disordered architecture because of their pseudosymmetric nature. In this work, we report a new 1D perovskite-like hybrid (MP) PbBr_3 (where MP is 1-methylpyrrolidinium), showing the near-room-temperature reversible switching of NLO properties. This material undergoes a solid-state NCS-to-CS structural phase transition at 316 K upon cooling, as confirmed

by differential scanning calorimetry (DSC) and dielectric measurements. At room temperature, strong SHG activities are observed in (MP)PbBr₃, which displays an intensity that is ~1.6 times as large as that of potassium dihydrogen phosphate. Strikingly, it can achieve the near-room-temperature reversible switching of SHG characteristics with a contrast of up to ~40 between its “SHG-on” and “SHG-off” states, which is beyond that of most thin films and their liquid counterparts^[34]. Further microscopic structural analyses reveal that the dynamic ordering of the organic MP⁺ cation and the inorganic chain-like skeleton triggers its centrosymmetric (*P6₃/mmc*) to acentric (*P2₁2₁2₁*) phase transition at 316 K upon cooling, which contribute to its NLO switching properties. This work shows the potential of (MP)PbBr₃ as a solid-state NLO switch and promotes the progress of NLO and NLO switching materials based on low-dimensional hybrid perovskites.

MATERIALS AND METHODS

Materials preparation

First, 2.53 g of lead acetate trihydrate (4 mmol) were added to a 100 mL round-bottomed flask, followed by 20 mL of a hydrobromic acid solution (40%) and 1.25 g of 1-methylpyrrolidine (3 mmol). They were then heated and stirred at 373 K for 1 h until all the precipitates were dissolved. The solvent was slowly evaporated at room temperature over several weeks and colorless crystals were obtained.

Structural characterization

Variable-temperature X-ray single-crystal diffraction analyses were carried out on a Bruker D8 diffractometer (Mo K α radiation, $\lambda = 0.71073$ Å) at 193 and 350 K, respectively. Powder X-ray diffraction (PXRD) data were collected on a Mini Flex 600 (Rigaku Co., Tokyo, Japan) diffractometer in the 2θ range of 5°–40° with a scan step of 0.02°.

Property measurements

A thermal analysis of the sample was carried out in the temperature range of 300–360 K. In the DSC experiments, the aluminum crucibles with the dry powder of (MP)PbBr₃ were put in a DSC instrument (NETZSCH 200 F3). Dielectric experiments were performed using an impedance analyzer (Tong Hui TH2828A). The SHG activities of (MP)PbBr₃ were investigated by applying the Kurtz-Perry model (Nd:YAG laser, $\lambda = 1064$ nm). Further details are available in the [Supplementary Material](#).

RESULTS AND DISCUSSION

Colorless crystals of (MP)PbBr₃ were obtained from the acidic solution through a slow evaporation process at room temperature. The phase purity of (MP)PbBr₃ was further verified by PXRD, which agrees reasonably well with the simulated pattern [[Supplementary Figure 1](#)]. Moreover, (MP)PbBr₃ is thermally stable below 584 K [[Supplementary Figure 2](#) and [Supplementary Table 1](#)]. Initially, the phase transition of (MP)PbBr₃ was detected by DSC and variable-temperature dielectric permittivity measurements. As depicted in [Figure 1A](#), a pair of endothermic and exothermic peaks are clearly observed at $T_c = 339$ and 316 K, respectively, in the process of heating and cooling, thereby revealing the reversible phase transition in (MP)PbBr₃. These sharp anomalous peaks and the large thermal hysteresis of ~23 K indicate that the phase transition should be of the first-order type. The corresponding enthalpy change (H) and entropy change (S) were calculated to be 12.69 J/g and 19.96 J/(mol·K) in the heating mode, respectively [[Supplementary Figure 3](#)]. A relatively small thermal anomaly was observed in the cooling run, probably due to the stepwise ordering of structural moieties. For convenience, the phases above and below T_c are designated as the high-temperature phase (HTP) and low-temperature phase (LTP), respectively. Furthermore, crystalline materials that show a thermally-induced structural phase transition usually display typical temperature-dependent dielectric responses^[35].

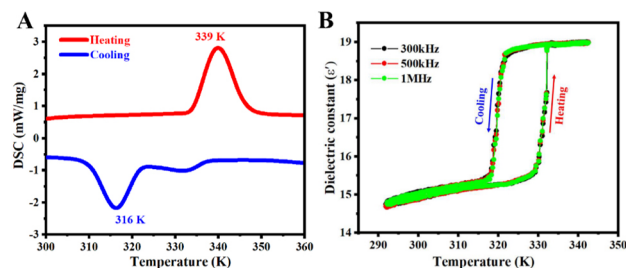


Figure 1. (A) DSC heating and cooling cycle measurements of (MP)PbBr₃. (B) Real part (ϵ') of dielectric constant in heating and cooling modes. DSC: Differential scanning calorimetry.

As shown in [Figure 1B](#), the temperature-dependent dielectric real part (ϵ') was measured at various frequencies (300 kHz–1 MHz), with two dielectric plateaus observed. For the LTP, the ϵ' values are ~ 15 and almost remain stable with the temperature variation. In the vicinity of T_c , the measured ϵ' rapidly increases to a plateau of ~ 19 , corresponding to the high-dielectric state of (MP)PbBr₃. The switching performance of the dielectric properties is reversible and displays a rectangular thermal hysteresis of ~ 20 K between the heating and cooling runs. Such dielectric bistability coincides well with the DSC traces, behaving as an indicator to the appearance of the phase transition.

For a deeper insight into the structural phase transition behavior, the single-crystal structures of (MP)PbBr₃ were collected at 350 K (above T_c , HTP) and 193 K (below T_c , LTP), respectively [[Supplementary Table 2](#)]. For the HTP, (MP)PbBr₃ crystallizes in a hexagonal crystal system with the CS space group $P6_3/mmc$. As shown in [Figure 2A](#), the asymmetric unit of the molecular structure contains an organic 1-methylpyrrolidinium cation and an inorganic [PbBr₃]⁻ component, which construct the ABX₃-type perovskite-like architecture. The 1D infinite chain-like frameworks consisting of the face-sharing PbBr₆ octahedra are almost aligned along the crystallographic c -axis direction [[Figure 2B](#)]. The most intuitive characteristic is the disordering of both the organic cations and inorganic scaffolds. The PbBr₆ inorganic octahedra adopt a highly-disordered configuration, as verified by the equivalent length of Pb-Br bonds (~ 3.0328 Å, [Supplementary Table 3](#)). Furthermore, organic MP⁺ cations also have the disordered molecular symmetry with six equivalent sites and closely link to the PbBr₆ octahedra skeleton through N-H \cdots Br hydrogen bonding interactions [[Figure 2A](#) and [Supplementary Figure 4](#)]. From the perspective of crystallography, the structural moieties locate at symmetric positions, thus satisfying the basic requirements of its CS symmetry.

When the temperature decreases below T_c , the symmetry of the crystal structure is broken. In the LTP, (MP)PbBr₃ transitions to the orthorhombic crystal system with the NCS space group $P2_12_12_1$ [[Supplementary Table 2](#)]. Furthermore, the basic molecular structure of (MP)PbBr₃ still contains one MP⁺ cation and one inorganic [PbBr₃]⁻ anion, which locate in completely ordered states. The 1D chain-like frameworks are composed of the face-sharing PbBr₆ octahedra extended along the a -axis direction [[Figure 2C](#) and [Supplementary Figure 4](#)]. However, the geometry of these 1D chain-like scaffolds is distorted during the structural phase transition, as verified by the unequal Pb-Br bond lengths of 2.8593–3.2076 Å [[Supplementary Table 3](#)]. Comparative studies of the variable-temperature crystal structures of (MP)PbBr₃ show that the dynamic ordering of the organic cations and inorganic frameworks affords the driving force to trigger its structural symmetry breaking at 316 K [[Figure 2C](#)]. The rotations and reorientations of such structural components make a dominant contribution to the generation of molecular dipole moments, as well as the macroscopic NLO properties. Therefore, it is expected that the NCS-to-CS phase transition of (MP)PbBr₃ will lead to NLO switching behavior.

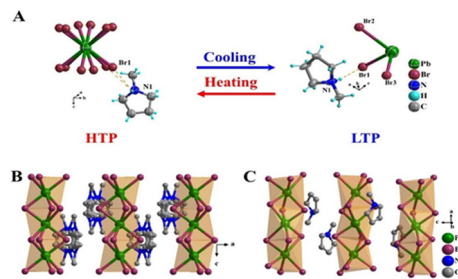


Figure 2. (A) Asymmetric units for molecular structures of (MP)PbBr₃ collected at 350 and 193 K, respectively. 1D packing structures of (MP)PbBr₃ in the (B) HTP and (C) LTP. Order-disorder changes are clearly observed during the phase transition. 1D: One-dimensional; HTP: high-temperature phase; LTP: low-temperature phase.

The above structural analyses demonstrate that the phase transition of (MP)PbBr₃ takes place from the centrosymmetric HTP ($P6_3/mmc$) to the non-centrosymmetric LTP ($P2_12_12_1$), leading to the notable breaking of crystallographic symmetry. Therefore, we analyzed the variations in the symmetry operation elements in (MP)PbBr₃ during its phase transition. As shown in Figure 3, there are 24 symmetric elements ($E, 2C_6, 2C_3, C_2, 3C'_2, 3C''_2, I, 2S_6, 2S_3, \sigma_h, 3\sigma_v$ and $3\sigma_d$) for the HTP, which dramatically decrease to 4 (E, C_2, σ_v and σ'_v) for the LTP^[36]. From the perspective of structural changes, it is the dynamic ordering of both the organic cations and inorganic chain-like scaffolds that give rise to the phase transition, along with the disappearance of the mirror planes and inversion center. Considering this structural change of (MP)PbBr₃, second-order NLO properties (e.g., SHG) would be expected in (MP)PbBr₃ for the LTP, as well as the solid-state switching of its SHG effects during the phase transition.

Consequently, we measured the SHG signals of (MP)PbBr₃ using the Kurtz-Perry method at room temperature. As shown in Figure 4A, the SHG signal intensities of (MP)PbBr₃ display a gradual enhancement with increasing particle size and become almost saturated, indicating the phase matching attribute of its NLO property. Compared with that of the KH₂PO₄ (KDP) reference in the same range of particle size, the SHG intensity of (MP)PbBr₃ is ~1.6 times greater (inset in Figure 4A and Supplementary Table 4), in good agreement with its NC structure in the LTP. Most intriguingly, the temperature-dependent reversible switching of the SHG intensities of (MP)PbBr₃ is observed, as depicted in Figure 4B. The SHG signals keep almost stable below ~335 K upon heating, corresponding to the “SHG-on” state. However, with the temperature continuing to increase, the SHG signals present a dramatic step-like decrease and then completely disappear above T_c , except for weak noise, which is termed the “SHG-off” state. This variation in SHG properties coincides with its structure changes during the phase transition. Taking the noise level as the reference, the “on/off” contrast for the switching quadratic NLO effects of (MP)PbBr₃ could be estimated to be at least 40, which is larger than those of the reported solid-state NLO-switching materials, such as (C₆H₁₄N)₂SbCl₅ (~13)^[37], NH₄[(CH₃)₄N]SO₄·H₂O (~24)^[38], (Hdabco⁺)(CF₃COO⁻) (~35)^[8] and (C₄H₁₆N₃)BiBr₆ (~35)^[39]. One of the most attractive attributes of (MP)PbBr₃ is the near-room-temperature phase transition point, in the vicinity of which its SHG signals demonstrate the most significant variation with respect to the temperature change. Compared with other solid NLO-switching counterparts, e.g., [(DPA)(18-crown-6)]ClO₄ (214 K)^[12], [C₄H₁₂NO]MnCl₃ (270 and 382 K)^[40] and [C₆H₁₁NH₃]₂CdCl₄ (215 and 367 K)^[41], this merit should be indicative of its application potential at room temperature.

Switching reversibility of the dielectric constant and NLO properties are also important to evaluate the application potential of solid-state switch materials^[42]. As shown in Figure 5A, the SHG effects of (MP)PbBr₃ can recover rapidly after six cycles without any attenuation during the repeated heating and

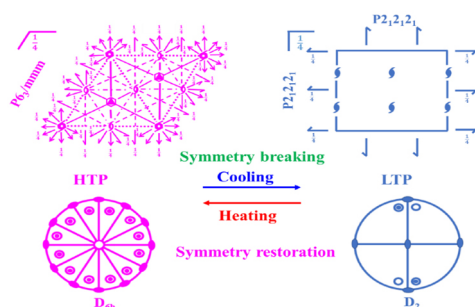


Figure 3. Transformation of spatial symmetry operations of (MP)PbBr₃ between the HTP ($P6_3/mmc$) and LTP ($P2_12_12_1$). HTP: High-temperature phase; LTP: low-temperature phase.

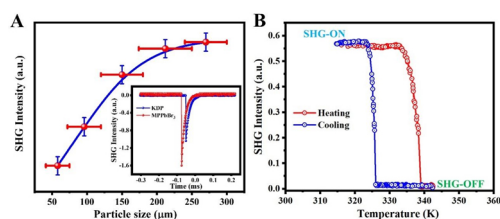


Figure 4. (A) Intensities of SHG signals versus crystal particle size of (MP)PbBr₃. Inset: SHG signals of (MP)PbBr₃ compared with KDP reference. (B) Temperature-dependent SHG intensities. SHG: Second harmonic generation.

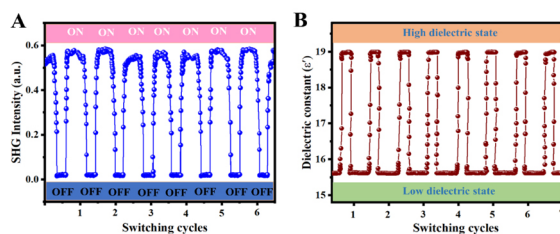


Figure 5. (A) Completely reversible and recoverable SHG switching. (B) Corresponding dielectric switching cycles in heating and cooling runs. SHG: Second harmonic generation.

cooling runs. A similar anti-fatigue merit is also observed in the dielectric measurements. With the temperature changing periodically, the corresponding ϵ' values demonstrate evident reversibility and remain quite stable after eight switching cycles [Figure 5B]. The superior reversibility figures of merit for (MP)PbBr₃ make it exhibit higher sensitivity and lower dissipation, which are essential for near-room-temperature solid-state NLO switching materials.

To illuminate the optical range for the potential NLO applications of (MP)PbBr₃, we measured its UV-Vis absorption spectrum at room temperature. As shown in Figure 6A, the optical absorption edge is located at 362 nm, corresponding to the bandgap of ~ 3.52 eV calculated from the *Tauc* equation (inset in Figure 6A). This bandgap value falls in the range of some values recently reported for 1D perovskite hybrids, such as [(CH₃)₃PCH₂F]PbBr₃ (3.215 eV)^[43] and [C₆H₁₄N]PbBr₃ (3.30 eV)^[44]. Since the physical properties of solid-state materials are closely related to their crystal and electronic structures^[45,46], we thus calculated the partial density of states of (MP)PbBr₃ to analyze its composition of electronic band structures [Supplementary Material]. Figure 6B shows that the H-1s states overlap with those of the C-2s/2p and N-2p orbitals, revealing that the C-H and N-H bonds of the organic moiety have strong covalent linkages.

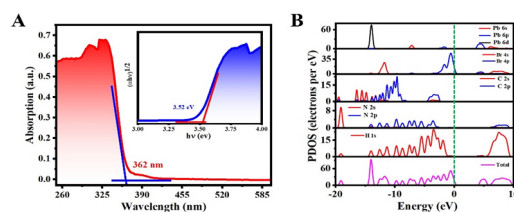


Figure 6. (A) UV-vis absorption spectrum of (MP)PbBr₃. Inset: bandgap calculated from *Tauc* equation. (B) Partial density of states analyses obtained from first-principles calculations.

However, the upper part of the valence bands is dominated by the Br-4*p* orbitals near the Fermi level and the bottom of the conduction bands involves the Pb-6*p* and Br-4*s/4p* orbitals. Obviously, both the maximum of the valence band and the minimum of the conduction band primarily originate from the Pb and Br atoms, and it is, therefore, the inorganic frameworks that determine the optical bandgap of (MP)PbBr₃. Considering the structural diversity of this organic-inorganic family, further optimization of the optical properties to a wide range could be achieved by modifying the inorganic components.

CONCLUSION

In summary, we have successfully obtained a one-dimensional perovskite-like hybrid, (MP)PbBr₃, which enables the near-room-temperature switching behavior of SHG properties. Microstructural analyses disclose that the dynamic ordering of the organic cations and inorganic networks leads to its CS-to-NCS symmetry breaking at 316 K. Strong quadratic NLO activities with an intensity ~1.6 times greater than that of KH₂PO₄ are verified in (MP)PbBr₃ in the LTP (termed the “SHG-on” state), while the SHG signals fully disappear above the *T_c* (“SHG-off” state). This NLO switching behavior demonstrates a large contrast of ~40 between the two different states, as well as notable switching repeatability. This work illustrates the excellent potential of (MP)PbBr₃ as an NLO material and also sheds light on the exploration of new NLO switching candidates in the family of hybrid perovskites.

DECLARATIONS

Acknowledgments

The authors thank Aurang Zeb for help with experimentation.

Authors' contributions

Synthesized and characterized the perovskite materials: Fan Q

Determined the single-crystal structures: Ma Y

Performed calculation and analysis: Liu Y

Implemented the characterization of the NLO material: Xu H, Song Y

Designed and directed the studies: Sun Z

Wrote the manuscript: Fan Q, Sun Z

Discussed the results and reviewed the manuscript: Fan Q, Ma Y, Xu H, Song Y, Liu Y, Luo J, Sun Z

Availability of data and materials

Not applicable.

Financial support and sponsorship

This work has been supported by NSFC (22125110, 21875251, 21833010, 22075285, and 21921001), the Key Research Program of Frontier Sciences of CAS (ZDBS-LY-SLH024), Fujian Science & Technology Innovation Laboratory for Optoelectronic Information of China (2021ZR126), the NSF of Fujian Province

(2020J01112), the Strategic Priority Research Program of CAS (XDB20010200), and the National Postdoctoral Program for Innovative Talents (BX2021315).

Conflicts of interest

All authors declared that there are no conflicts of interest.

Ethical approval and consent to participate

Not applicable.

Consent for publication

Not applicable.

Copyright

© The Author(s) 2022.

REFERENCES

1. Delaire JA, Nakatani K. Linear and nonlinear optical properties of photochromic molecules and materials. *Chem Rev* 2000;100:1817-46. DOI
2. Shi Y, Zhang C, Zhang H, et al. Low (Sub-1-volt) halfwave voltage polymeric electro-optic modulators achieved by controlling chromophore shape. *Science* 2000;288:119-22. DOI PubMed
3. Castet F, Rodriguez V, Pozzo JL, et al. Design and characterization of molecular nonlinear optical switches. *Acc Chem Res* 2013;46:2656-65. DOI PubMed
4. Boixel J, Guerschais V, Le Bozec H, et al. Second-order NLO switches from molecules to polymer films based on photochromic cyclometalated platinum(II) complexes. *J Am Chem Soc* 2014;136:5367-75. DOI
5. Coe BJ, Houbrechts S, Asselberghs I, Persoons A. Efficient, reversible redox-switching of molecular first hyperpolarizabilities in Ruthenium(II) complexes possessing large quadratic optical nonlinearities. *Angew Chem Int Ed* 1999;38:366-9. DOI
6. Li P, Wang M, Zhang M, et al. Electron-transfer photochromism to switch bulk second-order nonlinear optical properties with high contrast. *Angew Chem Int Ed* 2014;53:11529-31. DOI PubMed
7. van Bezouw S, Koo MJ, Lee SC, et al. Three-stage pH-switchable organic chromophores with large nonlinear optical responses and switching contrasts. *Chem Commun* 2018;54:7842-5. DOI PubMed
8. Sun Z, Luo J, Zhang S, et al. Solid-state reversible quadratic nonlinear optical molecular switch with an exceptionally large contrast. *Adv Mater* 2013;25:4159-63. DOI PubMed
9. Zeng Y, Hu C, Xu W, et al. An exceptional thermally induced four-state nonlinear optical switch arising from stepwise molecular dynamic changes in a new hybrid salt. *Angew Chem Int Ed* 2022;61:e202110082. DOI
10. Serra CP, van der Veen MA, Gobechiya E, et al. NH₂-MIL-53(Al): a high-contrast reversible solid-state nonlinear optical switch. *J Am Chem Soc* 2012;134:8314-7. DOI PubMed
11. Sun Z, Chen T, Liu X, Hong M, Luo J. Plastic transition to switch nonlinear optical properties showing the record high contrast in a single-component molecular crystal. *J Am Chem Soc* 2015;137:15660-3. DOI PubMed
12. Ji C, Sun Z, Zhang S, et al. A host-guest inclusion compound for reversible switching of quadratic nonlinear optical properties. *Chem Commun* 2015;51:2298-300. DOI PubMed
13. Chen T, Sun Z, Zhao S, et al. An organic-inorganic hybrid co-crystal complex as a high-performance solid-state nonlinear optical switch. *J Mater Chem C* 2016;4:266-71. DOI
14. Biswal BP, Valligatla S, Wang M, et al. Nonlinear optical switching in regioregular porphyrin covalent organic frameworks. *Angew Chem Int Ed* 2019;58:6896-900. DOI PubMed
15. Tao K, Wu Z, Han S, et al. Switchable behaviors of quadratic nonlinear optical properties originating from bi-step phase transitions in a molecule-based crystal. *J Mater Chem C* 2018;6:4150-5. DOI
16. Mei G, Zhang H, Liao W. A symmetry breaking phase transition-triggered high-temperature solid-state quadratic nonlinear optical switch coupled with a switchable dielectric constant in an organic-inorganic hybrid compound. *Chem Commun* 2016;52:11135-8. DOI PubMed
17. Zhang J, Han S, Liu X, et al. A lead-free perovskite-like hybrid with above-room-temperature switching of quadratic nonlinear optical properties. *Chem Commun* 2018;54:5614-7. DOI PubMed
18. Zheng X, Shi P, Lu Y, et al. Dielectric and nonlinear optical dual switching in an organic-inorganic hybrid relaxor [(CH₃)₃PCH₂OH][Cd(SCN)₃]. *Inorg Chem Front* 2017;4:1445-50. DOI
19. Shi P, Ye Q, Wang H, et al. Reversible phase transitions and dielectric properties in [(CH₃)₄P]₂[Cr₂O₇] and [Et₄P]₂[Cr₃O₁₀]. *Eur J Inorg Chem* 2015;2015:3255-63. DOI

20. Ma Y, Wang J, Guo W, et al. The first improper ferroelectric of 2D multilayered hybrid perovskite enabling strong tunable polarization-directed second harmonic generation effect. *Adv Funct Mater* 2021;37:2103012. DOI
21. Xu G, Zhang W, Ma X, et al. Coexistence of magnetic and electric orderings in the metal-formate frameworks of $[\text{NH}_4][\text{M}(\text{HCOO})_3]$. *J Am Chem Soc* 2011;133:14948-51. DOI
22. Du Z, Xu T, Huang B, et al. Switchable guest molecular dynamics in a perovskite-like coordination polymer toward sensitive thermoresponsive dielectric materials. *Angew Chem Int Ed* 2015;54:914-8. DOI PubMed
23. Shi C, Zhang X, Cai Y, et al. A chemically triggered and thermally switched dielectric constant transition in a metal cyanide based crystal. *Angew Chem Int Ed* 2015;54:6206-10. DOI PubMed
24. Shi D, Adinolfi V, Comin R, et al. Low trap-state density and long carrier diffusion in organolead trihalide perovskite single crystals. *Science* 2015;347:519-22. DOI PubMed
25. Liu X, Ji C, Wu Z, et al. $[\text{C}_5\text{H}_{12}\text{N}]\text{SnCl}_3$: A Tin halide organic-inorganic hybrid as an above-room-temperature solid-state nonlinear optical switch. *Chem Eur J* 2019;25:2610-5. DOI
26. Xu W, He C, Ji C, et al. Molecular dynamics of flexible polar cations in a variable confined space: toward exceptional two-step nonlinear optical switches. *Adv Mater* 2016;28:5886-90. DOI PubMed
27. Zhou Q, Wang L, Xu Q, et al. Effective cleanup of oil contamination on bio-inspired superhydrophobic surface. *Environ Sci Pollut Res* 2019;26:21321-8. DOI PubMed
28. Zhang W, Xiong R. Ferroelectric metal-organic frameworks. *Chem Rev* 2012;112:1163-95. DOI PubMed
29. Saparov B, Mitzi DB. Organic-inorganic perovskites: structural versatility for functional materials design. *Chem Rev* 2016;116:4558-96. DOI PubMed
30. You Y, Liao W, Zhao D, et al. An organic-inorganic perovskite ferroelectric with large piezoelectric response. *Science* 2017;357:306-9. DOI PubMed
31. Ai Y, Sun R, Zeng Y, et al. Coexistence of magnetic and electric orderings in a divalent Cr^{2+} -based multiaxial molecular ferroelectric. *Chem Sci* 2021;12:9742-7. DOI PubMed PMC
32. Sun Z, Zeb A, Liu S, et al. Exploring a lead-free semiconducting hybrid ferroelectric with a zero-dimensional perovskite-like structure. *Angew Chem Int Ed* 2016;128:12033-7. DOI PubMed
33. Ji C, Wang S, Liu S, et al. Exceptional three-level switching behaviors of quadratic nonlinear optical properties in a tristable molecule-based dielectric. *Chem Mater* 2017;29:3251-6. DOI
34. Sun Z, Li S, Zhang S, et al. Second-order nonlinear optical switch of a new hydrogen-bonded supramolecular crystal with a high laser-induced damage threshold. *Adv Optical Mater* 2014;2:1199-205. DOI
35. Zhang Y, Ye H, Fu D, et al. An order-disorder ferroelectric host-guest inclusion compound. *Angew Chem Int Ed* 2014;53:2114-8. DOI PubMed
36. Penfold D, Dacombe M, Barnes S, Ashcroft N. International tables for crystallography. 5rd ed. Cham: Springer; 2005; pp. 10-834.
37. Zhang J, Sun Z, Zhang W, et al. Hydrogen-bonded switchable dielectric material showing the bistability of second-order nonlinear optical properties. *Cryst Growth Des* 2017;17:3250-6. DOI
38. Liu S, Sun Z, Ji C, et al. Exceptional bi-step switching of quadratic nonlinear optical properties in a one-dimensional channel compound. *Chem Commun* 2017;53:7669-72. DOI PubMed
39. Wu Z, Liu X, Ji C, et al. Above-room-temperature switching of quadratic nonlinear optical properties in a Bi-halide organic-inorganic hybrid. *J Mater Chem C* 2018;6:9532-6. DOI
40. Hua X, Zhang W, Shi P. Two-step nonlinear optical switch in a hydrogen-bonded perovskite-type crystal. *Chem Commun* 2022;58:1712-5. DOI
41. Liao W, Ye H, Fu D, et al. Temperature-triggered reversible dielectric and nonlinear optical switch based on the one-dimensional organic-inorganic hybrid phase transition compound $[\text{C}_6\text{H}_{11}\text{NH}_3]_2\text{CdCl}_4$. *Inorg Chem* 2014;53:11146-51. DOI PubMed
42. Peng H, Liu Y, Huang X, et al. Homochiral one-dimensional ABX_3 lead halide perovskites with high- T_c . *J Mater Chem C* 2017;5:4756-63. DOI
43. Cao Y, Zhou L, He L, et al. Phase transition and band gap regulation by halogen substituents on the organic cation in organic-inorganic hybrid perovskite semiconductors. *Chem Eur J* 2020;26:14124-9. DOI
44. Zhang J, Liu X, Li X, et al. $[\text{C}_6\text{H}_{14}\text{N}]\text{PbBr}_3$: An ABX_3 -type semiconducting perovskite hybrid with above-room-temperature phase transition. *Chem Asian J* 2018;13:982-8. DOI
45. Li P, Tang Y, Liao W, et al. A semiconducting molecular ferroelectric with a bandgap much lower than that of BiFeO_3 . *NPG Asia Mater* 2017;9:e342. DOI
46. Chen Y, Gao C, Yang T, et al. Research advances of ferroelectric semiconductors of 2D hybrid perovskites toward photoelectronic applications. *Chin J Struct Chem* 2022;41:2204001-11. DOI